Verification of two-dimensional numerical earthquake site effects on a dam site, Costa Rica

C. Sigarán-Loría & R. Hack
Department of Earth Systems Analyses, ITC, Enschede, The Netherlands

ABSTRACT: The ground response and site effects of a steep valley were verified with a two dimensional plane strain analysis in the time domain against recorded motions. Weak motions (<0.15 g) have been measured on the site with three accelerographs placed at the base and crests of the slopes. The instrument at the base is on rock and the ones towards the crests on soil. Dynamic models were done with the finite element method (*FEM*), loading at the base the signals recorded on rock. The peak ground accelerations (*PGA*) obtained with the *FEM* fit with the ones measured *in situ*. The comparison between the main frequencies of the events and the fundamental frequencies of the site show resonance effects. The raised amplifications were demonstrated to be caused by geological site effects, related to the upper geotechnical unit and not by the topography. These results show the importance of subsurface structure in causing resonance effects.

1 INTRODUCTION

Numerical methods have been recently applied for back and parametric analysis of earthquake ground response and site effects (e.g. Athanasopoulos et al., 1999; Havenith et al., 2002; Lokmer et al., 2002; Paolucci, 2002; Papalou & Bielak, 2004; Bouckovalas & Papadimitriou, 2005; Psarropoulos et al., 2007). There are few attempts to verify measured with modelled data in time and frequency domains accounting for topographic and geologic effects separately (e.g. Semblat et al., 2005; Assimaki et al., 2005). Thimus et al. (2006) present a theoretical verification of wave propagation with finite differences (*FDM*). Sincraian & Oliveira (2001) had field measurements but could not find a good fit with the *2-* and *3D FEM* they used. Geli et al. (1988) found that *2D* models underestimate field observations, caused by the simplicity of the models. Only the 3D model in frequency domain showed a good match. They concluded that for peak ground accelerations (*PGA*) smaller than 0.24 g hills behave approximately linear.

Users of these tools should be aware of the limits of their applicability and benchmark results. Weak motions have been validated with field data with a *3D* hybrid approach (indirect boundary elements method) by LeBrun et al. (1999). They found a good correlation on the responses for frequencies lower than 1 Hz. On the other hand, *1-D* analysis methods have been extensively verified as documented by Kramer & Stewart (2004) with nearby rock-soil signals as well as vertical arrays.

Strong amplifications have been measured in some cases on hills (Bouchon & Barker, 1996) and related to topographical site effects, without quantifying the effects of the local geology.

This paper presents the comparison of the ground responses modelled with two-dimensional (*2D*) linear elastic finite elements (*FEM*) of a site with field measurements, comparing the site effects of topography and geology. The site is located in a highly seismic region of Costa Rica.

2 ADDRESSED PROBLEM

Two-dimensional (*2D*) plane strain numerical models with *FEM* were used to verificate the ground response and site effects of an instrumented site with *in situ* recorded weak motions (*PGA*<0.15 g) in time domain.

The location was a dam site in a steep valley, mainly consisting of rock with a transitional weathering profile towards a saprolitic type of material on top. This project is located in a highly seismic region in Costa Rica, at the central Pacific side, along the fore-arc region (Figure 1). The main seismic sources are the Meso-American subduction trench (inter-plate) along the Pacific, as well as local faulting (intra-plate).

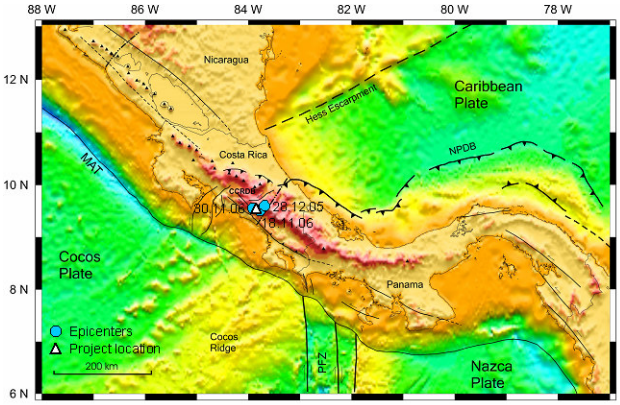

Figure 1. Geotectonic setting of Costa Rica (modified after Flueh & von Huene, 2007).

3 FIELD MEASUREMENTS & MODELS

3.1 *Field measurements*

Three digital Etna Kinemetrics accelerographs have been registering motions on the site since September 2005. One is at the base of the valley on rock, and one at each abutment

towards each slope crest, on saprolitic materials (highly weathered rock), at heights of 190 m and 135 m above the river. They were aligned with a North-South (*NS*) strike, parallel to the dam axis (

Figure **2**).

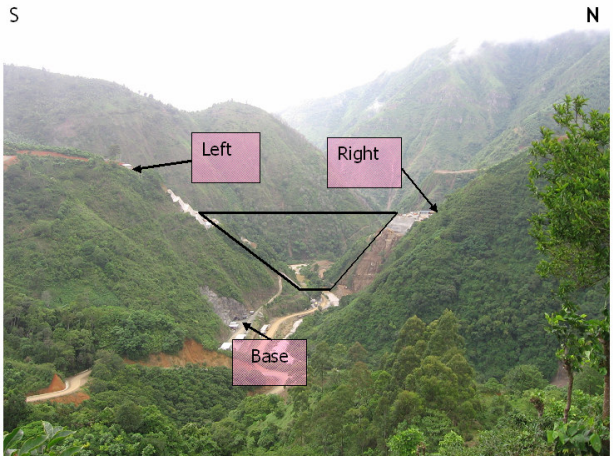

Figure 2. Dam site looking in downstream direction with sketch of dam and accelerographs placement.

These instruments have a register capacity of 2 g amplitude, and a frequency range from 0.12 Hz to 45 Hz. Some weak motions have been registered, from which three near-field events were chosen for this analyses (Table 1).

Table 1. Characteristics of the measured earthquakes

Event date	Magnitude (Mw)	Source of rupture	Hypocentral depth (km)	Distance & direction from dam (km)
28/12/2005	5.1	Subduction	43	24.2 *NW*
18/11/2006	5.0	Local fault	23.8	6.5 *SW*
30/11/2006	4.8	Local fault	9	23 *W*

The responses at the measurement points are listed in Table 2, with the main frequencies obtained from smoothed Fourier amplitude spectra. The left slope is not registered on the last motions due to a defect on that accelerograph.

Table 2. Site responses and Fourier spectra frequencies

Event / Station	Peak ground acceleration (*PGA*) (cm/s^2)			Fourier spectra (Hz)
	NS	EW	Vertical	
28.12.2005				
Base	10.99	16.82	9.53	1-10
Right crest	129.26	82.91	39.25	4
Left crest	120.18	120.15	58.05	3
18.11.2006				
Base	7.26	16.02	6.42	3-10
Right crest	40.96	40.91	33.79	4-5
30.11.2006				
Base	3.94	8.80	3.66	1-9
Right crest	20.75	18.84	13.91	4-6

The rock motions ("base" signals) from the *NS* component were the input for the numerical models The three events had base-line correction, the same frequency range (0.12-45 Hz) and duration (about 20 s each).

3.2 *The 2-D FEM models*

All the *FEM* models from the valley had the same dimensions and mesh coarseness. The elements used were 15-noded triangular, fine enough to insure appropriate wave propagation in accordance with the wavelength and shear wave velocities of the materials. The models were further refined towards the surface.

The distances from the boundaries were: from the slope crests to the lateral boundaries approximately 1300 m and from the base of the valley to the bottom boundary 20 m depth. They were chosen after a sensitivity assessment of the site response under different dynamic loads to find the models for which the responses converge, avoiding possible reflections from the boundaries.

The responses in the models were measured at different points to control the amplification patterns but the focus of this paper is on the points that correspond with the accelerograph locations. These are shown in Figure 3. "L" is the accelerograph from the left slope, corresponding with the slope crest, and "R" the one at the right slope, located approximately 90 m behind the slope crest.

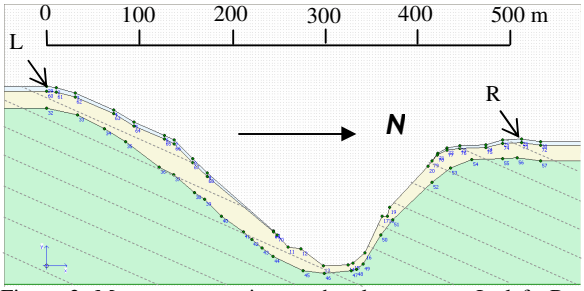

Figure 3. Measurement points at the slope crests, L: left, R: right (equal horizontal and vertical scales) and apparent dip of the layers.

3.3 *Ground properties and constitutive model*

The site consists of a discontinuous rock mass of turbidites (sandstones and shales), of an Oligo-Miocene Formation (Térraba Formation). The average bedding is 290°/25° dipping downstream (Figure 3). Geotechnically, it is divided in three units: (a) lower: slightly-weathered rock, (b) intermediate: moderately weathered and decompressed rock and (c) upper: completely weathered, transitional to soil (saprolite). The lower unit is found at 23 m depth in the left abutment and 20 in the right approximately. It transitionally turns into the intermediate unit, which has about 18 and 16.5 m thickness on the left and right abutments respectively. The upper unit (saprolitic material) is considerably weaker and less stiff. Its thickness is 5 and 4 m on the left and right abutments correspondingly, at the accelerographs locations. The spatial distribution of the units is sketched in Figure 3, and their properties are summarized in Table 3. The geotechnical characterization was done through extensive *in situ* and laboratory tests (e.g. plate bearing, SPT, triaxial), geophysical (e.g. microseismicity, seismic refraction) and geological (e.g. drillcore, mapping) survey.

The left slope has a steepness of 43° and 36° towards the crest. It is gentler than the right slope due to the bedding dip and strike angles towards the river in that side. The opposite happens on the right abutment, giving higher steepness to the slope (57° to 50°).

Due to the scale of this analysis, the complexity of the discontinuities characterization, nonlinearity, heterogeneity and anisotropy of the rock mass could not be incorporated in the models. In the models the site was considered as a homogeneous, isotropic continuum. The properties were used following Table 3.

Table 3. Geotechnical parameters of the site

Parameter	Name	Unit	Geotechnical Units		
			Upper	Intermediate	Lower
Material model	*Model*	-	Linear elastic		
Material behaviour	*Type*	-	Drained		
Unit weight	γ	kN/m^3	18	26.5	27.1
Young's modulus	E_{ref}	kPa	5e+4	2.5e+6	7e+6
Poisson's ratio	ν	-	0.3	0.3	0.25
Shear wave velocity	v_s	m/s	102	596	1006
Wavelength for highest frequency	λ	m	2.3	13.2	22.4
Rayleigh damping constants	α	-	0.0314	0.0314	0.0314
	β	-	3.2e-4	3.2e-4	3.2e-4

As the strains for these types of events are small, deformations range within the elastic range. Therefore, the linear elastic model was suitable for the purpose of this analysis.

Different geological-geotechnical scenarios were evaluated to discern between the geological and topographical site effects and to quantify it. This was done with a model with the site topography and without the upper geotechnical unit. This unit was substituted with the intermediate unit, giving this model two units. Another evaluation was made with only the lower unit.

3.4 *Dynamic properties and loads*

Dynamic viscous absorbent boundaries were used to avoid reflections. The horizontal *NS* component of the registered acceleration time histories from the base station on rock were prescribed along the bottom boundary. The peak accelerations and main frequencies of the input signals are given in Table 2.

The damping of the system was Rayleigh type, chosen for the frequency band of the input signals. The resultant mass (α) and stiffness (β) proportional constants were estimated for a 5% damping (Table 3).

The natural frequencies of the site were estimated from transfer functions on a one-dimensional equivalent-linear system with different earthquake signals from the world given by the software. The right side displayed a first oscillation mode between 5 and 6 Hz and a second around 9.5 Hz. The left side had the first oscillation mode between 3.5 and 4.4 Hz, and a second around 8.5 Hz. The left slope has a slightly lower fundamental frequency due to the thicker upper unit of the saprolite. The result of the right slope are shown in Figure 4.

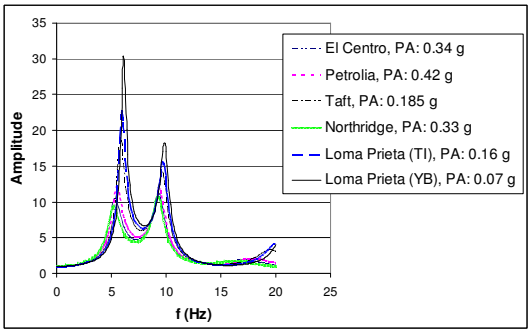

Figure 4. Oscillation modes at the accelerograph location at the right slope.

4 *2-D FEM* GROUND RESPONSES

The site responses from the *FEM* models were measured behind the crests of both slopes and along the slope at the left margin. The outputs from the points that correspond with the accelerographs locations are listed in Table 4. The strongest registered motion (December 28, 2005) was also modeled with variations in the geology, keeping the site topography to quantify the site effect of geology on the response (Table 4).

Table 4. Peak ground accelerations and amplification factors at the right and left crests

Event	Right crest *PGA* (cm/s^2)	A.f.*	Left crest *PGA* (cm/s^2)	A.f.
28.12.2005	127.6	11.6	118.8	10.8
2 units	36.9	3.4	29.1	2.6
1 unit	28.8	2.6	32.0	2.9
18.11.2006	43.3	5.9	53.3	7.3
30.11.2006	25.8	6.5	28.9	7.3

*A.f: amplification factor

4.1 *Amplitude*

The peak ground accelerations of the site under the three motions are given in Table 4 and Figure 5. A good match in amplitude between the field measurements (referred as "instr.") and the responses from the numerical models was obtained. Figure 6 illustrates the spatial distribution of the horizontal accelerations on the left slope.

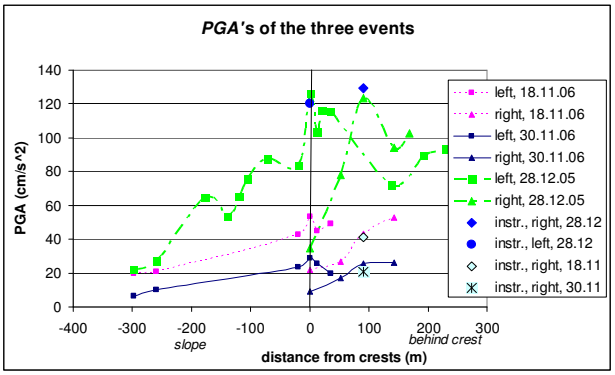

Figure 5. Peak ground accelerations of the three motions along the left slope and behind the crests of both slopes. The cero on the "x" axis represents the crest of each slope. "Instr." are the instrumental field measurements.

For the left slope, a consistent trend of higher amplification towards the slope crest was obtained coinciding with the position of the accelerograph (Figure 5 and Figure 6). The right slope showed a peak around 100 m from the crest for the stronger event (approximate location of the accelerograph, described in 3.1.2), but for the other two motions that trend was not clear (Figure 5). More measurement points are needed to make further conclusions.

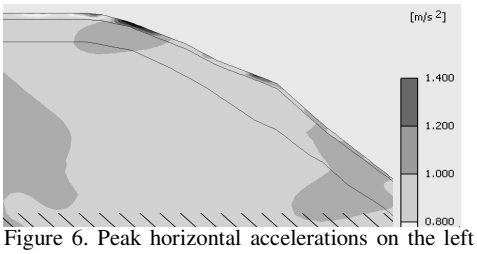

Figure 6. Peak horizontal accelerations on the left slope (in m/s^2). Peak towards the crest. Response under the motion of 28.12.2005.

When overlapping the time domain outputs from the model with the accelerographs signals, it was found a good correspondence for the stronger event (28.12.2005), but the others showed a time disparity of 2 to 4 s, although the signals kept similar shapes amongst them.

4.2 *Site effects on the amplification*

Three models with variations in the geotechnical units keeping the site topography were assessed to quantify the amplification associated to the geological site effect.

The two-units model was performed without the upper unit (saprolite). That layer was substituted with the material of the intermediate unit. Similarly, the one-layer model was carried out considering only the response of the lower unit within the site morphology. The peak accelerations and amplification factors of these models are given in Table 4. As expected, the model with one unit model gave the lowest amplifications, followed by the two-units one. The difference between the responses of these models with the real situation (three units) is important. When removing the upper unit, the amplification factors drop down 3.4 to 4 times, from 11.6 to 3.4 in the right slope, and from 10.8 to 2.6 in the left (Table 4). The removed layer has important differences in its physical-mechanical properties and lower impedance. The one-unit model displayed similar range and trend in its responses to the two-units one (Table 4).

Locally, below the accelerographs locations, the fundamental frequencies were estimated as 5-6 Hz at the right side and 3.5-4.4 Hz at the left side (Figure 4). The frequency content of the Fourier spectra (Table 2) of the three events showed a similar range between 1 and 10 Hz at the base. The same spectra at the accelerographs locations displayed a main frequency peak between 4-6 Hz at the right slope and 3 Hz at the left. Comparing the Fourier amplitude spectrum of the site with the fundamental natural frequencies, it is seen that under those places resonance develops in the upper geotechnical unit.

5 CONCLUSIONS

The numerical ground responses of this plane strain survey provided a good approximation of three field measured weak earthquakes (<0.15g) in time domain, applying the linear elastic material model. The magnitudes of the amplitudes got from the models gave a good fit to reality, despite the restrictions two dimensions induce on wave propagation for spatial analyses of ground response and site effects, besides the local geotechnical complexities (nonlinear behaviour, heterogeneity, etc.).

The high amplification ratios measured on the site (10 to 12 at the slope crests for the stronger motion), are related to a resonance development in the upper unit due to geological site effect. The fundamental site frequencies and main frequencies of the events coincide, and the geotechnical properties suggest a high impedance difference between the units, being greatly lower for the upper unit. This was clear from the model without the upper unit ("two layers"), below the accelerographs locations. On that model the amplifications decreased 3.4 to 4 times to factors of 2.6 to 3.4.

6 AKNOWLEDGEMENTS

The first author would like to express her gratitude to the Costar Rican Electricity Institute (ICE) for the support with the fieldwork, instrumentation and data for these analyses. In special to A. Climent and M. Jiménez. To A. Kaynia from the Norwegian Geotechnical Institute (NGI) for his remarks and R. Brinkgreve from PLAXIS for his support. This research is sponsored by the Strengthening Local Authorities in Risk Management (SLARIM) project of ITC, The Netherlands.

7 REFERENCES

Assimaki, D., Gazetas, G., Kausel, E. 2005. Effects of local soil conditions on the topographic aggravation of seismic motion: Parametric investigation and recorded field evidence from the 1999 Athens earthquake. *Bulletin of the Seismological Society of America*, 95(3): 1059-1089.

Athanasopoulus, G.A., Pelekis, P.C., Leonidou, E.A. 1999. Effects of surface topography on seismic ground response in the Egion (Greece) 15 June 1995 earthquake. *Soil Dynamics and Earthquake Engineering*, 18: 135-149.

Bouchon, M. & Barker, J.S. 1996. Seismic response of a hill: The example of Tarzana, California. *Bulletin of the Seismological Society of America*, 86(1A): 66-72.

Bouckovalas, G.D. & Papadimitriou, A.G. 2005. Numerical evaluation of slope topography effects on seismic ground motion. *Soil Dynamics and Earthquake Engineering*, 25: 547-558.

Flueh, E.R. & Huene, R. 2007. Crustal structure. In J. Bundschuh & G.E. Alvarado (eds.), *Central America: Geology, Resources and Hazards*: 123-158, ch. 10. Rotterdam: Balkema.

Geli, L., Bard, P.-Y., Jullien, B. 1988. The effect of topography on earthquake ground motion: A review and new results. *Bulletin of the Seismological Society of America*, 78: 42-63.

Havenith, H.-B., Jongmans, D., Faccioli, E., Abdrakhmatov, K., Bard, P.-Y. 2002. Site effect analysis around the seismically induced Ananevo rockslide, Kyrgyzstan. *Bulletin of the Seismological Society of America*, 92(8): 3190-3209.

Kramer, S.L. & Stewart, J.P. 2004. Geotechnical aspects of seismic hazards. In Y. Bozorgnia & V.V. Bertero (eds.), *Earthquake Engineering: form Engineering Seismology to Performance-Based Engineering*: 85 pp., ch. 4, USA: CRC Press.

LeBrun, B., Hatzfeld, D., Bard, P.Y., Bouchon, M. 1999. Experimental study of the ground motion on a large scale topographic hill at Kitherion (Greece). *Journal of Seismology*, 3_1-15.

Lokmer, I., Herak, M., Panza, G.F., Vaccari, F. 2002. Amplification of strong ground motion in the city of Zagreb, Croatia, estimated by computation of synthetic seismograms. *Soil Dynamics and Earthquake Engineering*, 22:105-113.

Paolucci, R. 2002. Amplification of earthquake ground motion by steep topographic irregularities. *Earthquake Engineering and Structural Dynamics*, 31:1831-1853.

Papalou, A. & Bielak, J. 2004. Nonlinear seismic response of earth dams with canyon interaction. *Journal of Geotechnical and Geoenvironmental Engineering, ASCE*, January: 103-110.

Psarropoulos, P.N., Tsompanakis, Y., Karabatsos, Y. 2007. Effects of local site conditions on the seismic response of municipal solid waste landfills. *Soil Dynamics and Earthquake Engineering*, 27: 553-563.

Semblat, J.F., Kham, M., Parara, E., Bard, P.Y., Pitilakis, K., Makra, K., Raptakis, D. 2005. Seismic wave amplification: Basin geometry vs soil layering. *Soil Dynamics and Earthquake Engineering*, 25: 529-538.

Sincraian, M.V. & Oliveira, C.S. 2001. A 2-D sensitivity study of the dynamic behavior of a volcanic hill in the Azores Islands: Comparison with 1-D and 3-D models. *Pure and Applied Geophysics*, 158: 2431-2450.

Thimus, J.-F., Delvosal, P., Waltener, S., Schroeder, C., Boukpeti, N. 2006. Analysis of seismic wave propagation in soils. In P. Verona & R. Hart (eds.), *FLAC and Numerical Modeling in Geomechanics – 2006*, Proceedings of the 4th International FLAC Symposium, 29-31 May 2006: 181-186, Madrid, Minnesota: ITASCA Consulting Group, Inc.